Supporting Information

Regioselective *ortho* Amination of Coordinated 2-(Arylazo)pyridine. Isolation of Air-Stable Monoradical Palladium Complexes of a New Series of Azo-Aromatic Pincer Ligands

Debabrata Sengupta,[†] Nabanita Saha Chowdhury,[†] Subhas Samanta,[†, ◊, #] Pradip Ghosh,[†] Saikat Kumar Seth, [§] Serhiy Demeshko,[#] Franc Meyer[#] and Sreebrata Goswami[†,*]

[†]Department of Inorganic Chemistry, Indian Association for the Cultivation of Science, Jadavpur, Kolkata 700 032

[◊]Department of Chemical Sciences, Indian Institute of Science Education and Research Kolkata, Mohanpur 741246, Nadia, India

[#]Institut für Anorganische Chemie, Georg-August-Universität Göttingen, Tammannstraße 4, 37077 Göttingen, Germany

[§] Department of Physics, Mugberia G. Mahavidyalaya, Bhupatinagar, Purba Medinipur 721425, India

Table S1. Cyclic voltammetry data[a,b] of [Pd(L^{1a-1f})Cl_2].

Compound	$E_{1/2}$ [c], V (ΔE_p, mV)
Pd(L^{1a})Cl_2	-0.155 (80), -0.91 (150)
Pd(L^{1b})Cl_2	-0.095 (80), -0.85 (100)
Pd(L^{1c})Cl_2	-0.100 (85), -0.90 (100)
Pd(L^{1d})Cl_2	-0.005 (80), -0.92 (150)
Pd(L^{1e})Cl_2	-0.19 (75), -0.93[d]
Pd(L^{1f})Cl_2	-0.49,[d] -0.90 (100)

[a]In a acetonitrile solution, supporting electrolyte Et_4NClO_4 (0.1 M), and reference electrode Ag/AgCl. [b]Solute concentration *ca*. 10^{-3} M. [c]$E_{1/2} = 0.5(E_{pa} + E_{pc})$, where E_{pa} and E_{pc} are anodic and cathodic peak potentials, respectively; $\Delta E_p = E_{pa} - E_{pc}$; scan rate = 50 mV s^{-1}. [d]Quasi-reversible.

Table S2. Cyclic voltammetry Data[a,b] of **1a – 1h**.

Compound	**Oxidation [$E_{1/2}^{c}$, (ΔE_p, mV)]**	**Reduction [$E_{1/2}^{c}$, V(ΔE_p, mV)]**
1a	0.25 (75)	- 0.66 (80)
1b	0.31 (80)	- 0.64 (85)
1c	0.21 (80)	- 0.68 (90)
1d	0.21 (85)	- 0.70 (85)
1e	0.32 (80)	- 0.76 (85)
1f	0.20 (85)	- 0.82 (85)
1g	0.17 (85)	- 0.83 (80)
1h	0.20 (80)	- 0.80 (90)

[a]In a dichloromethane solution, supporting electrolyte Bu_4NClO_4 (0.1 M), and reference electrode SCE. [b]Solute concentration ca. 10^{-3} M. [c]$E_{1/2} = 0.5(E_{pa} + E_{pc})$, where E_{pa} and E_{pc} are anodic and cathodic peak potentials, respectively; $\Delta E_p = E_{pa} - E_{pc}$; scan rate = 50 mV s^{-1}.

Table S3. UV-Vis NIR spectral transitions of coloumetrically generated **1c**, $[\mathbf{1c}]^+$ and $[\mathbf{1c}]^-$.

Compound	**Electronic Spectra**		
1c	**Experimental λ/nm (ε x 10^{-4})**	**Calculated λ/nm (f)**	**Contribution**
	575 (3894)	511 (0.118)	HOMO (β) →LUMO (β) (85%)
	390 (7462)	392 (0.018)	HOMO-3 (β) → LUMO (β) (33%), HOMO-2 (β) → LUMO (β) (30%)
	348 (8384)	356 (0.209)	HOMO (α) →LUMO+3 (α) (14%), HOMO-8 (β) → LUMO (β) (17%)
$[1c]^-$	506 (3533)	459 (0.064)	HOMO →LUMO+1 (84%)
	395 (2159)	352 (0.141)	HOMO → LUMO+6 (48%)
	305 (10526)	326 (0.150)	HOMO →LUMO+7 (36%), HOMO → LUMO+8 (45%)
	280 (11191)	282 (0.127)	HOMO-6 →LUMO (38%), HOMO-3 →LUMO(25%)
$[1c]^+$	580 (2920)	596 (0.016)	HOMO →LUMO (90%)
	433 (4558)	411 (0.184)	HOMO-4 → LUMO (57%)
	367 (16262)	366 (0.140)	HOMO-7 →LUMO (59%)

Table S4. UV-Vis NIR spectral transitions of the coloumetrically generated $[Pd(L^{1a\text{-}1f})Cl_2]^-$ in acetonitrile solution.

Compound	**Electronic Spectra**		
$[Pd(L^{1a})Cl_2]^-$	**Experimental λ/nm (ε x 10^{-4})**	**Calculated λ/nm (f)**	**Contribution**
	550 (0.17)	511 (0.016)	HOMO (α) →LUMO (α) (17%), HOMO-1 (β) → LUMO (β) (40%)
	340 (1.40)	326 (0.145)	HOMO-4 (β) → LUMO (β) (36%)
	269 (2.14)	--	--
$[Pd(L^{1b})Cl_2]^-$	560 (0.17)	511 (0.022)	HOMO (α) →LUMO (α) (23%), HOMO-1 (β) → LUMO (β) (38%)
	375 (0.90)	340 (0.15)	HOMO-4 (β) → LUMO (β) (29%)
	270 (2.69)	--	--
$[Pd(L^{1c})Cl_2]^-$	566 (0.12)	500 (0.26)	HOMO (α) →LUMO (α) (23%), HOMO-1 (β) → LUMO (β) (53%)
	376 (0.79)	335 (0.59)	HOMO-4 (β) → LUMO (β) (36%)
	256 (1.66)	--	--
$[Pd(L^{1d})Cl_2]^-$	590 (0.08)	553 (0.0017)	HOMO (α) →LUMO (α) (86%), HOMO (α) → LUMO + 4(α) (3%)
	390 (0.96)	371 (0.0432)	HOMO-6 (β) → LUMO (β) (43%)
	270 (1.79)	309 (0.0418)	HOMO-2 (α) →LUMO (α) (15%), HOMO-8 (β) → LUMO (β) (14%)
$[Pd(L^{1e})Cl_2]^-$	535 (0.15)	512 (0.156)	HOMO (α) →LUMO (α) (15%), HOMO-1 (β) → LUMO (β) (40%)
	320 (0.64)	327 (0.115)	HOMO-4 (β) → LUMO (β) (26%)
	257 (2.01)	--	--

Table S5. Crystallographic data of the complexes **1c**, **1e**, **1f**, **1h** and **Pd-I**.

	1c	**1e**	**1f**	**1h**	**Pd-I**
empirical formula	$C_{18}H_{16}ClN_4Pd$	$C_{15}H_{17}Cl_2N_4Pd$	$C_{18}H_{15}Cl_2N_4Pd$	$C_{13}H_{13}Cl_2N_4Pd$	$C_{47}\ H_{37}\ Cl_2\ N_3\ P_2\ Pd$
molecular mass	430.20	430.63	464.64	402.57	883.04
temperature (K)	120	150	150	150	293
crystal system	Monoclinic	Monoclinic	Triclinic	Triclinic	Triclinic
space group	C2/c	P21/c	P-1	P-1	P-1
a (Å)	19.819(3)	7.6921(17)	7.245(5)	10.540(5)	10.669(5)
b (Å)	10.3894(13)	11.836(3)	9.789(5)	10.890(5)	12.002(5)
c (Å)	18.274(4)	18.457(4)	12.606(5)	12.786(5)	16.139(5)
α(deg)	90	90	91.937(5)	96.823(5)	80.675(5)
β (deg)	118.773(2)	95.398(4)	91.401(5)	97.327(5)	82.573(5)
γ (deg)	90	90	91.477(5)	95.295(5)	89.627(5)
V ($Å^3$)	3298.2(10)	1672.9(7)	892.9(8)	1436.7(11)	2022.0(14)
Z	8	4	2	4	2
D_{calcd} (g/cm^3)	1.733	1.710	1.728	1.861	1.450
cryst. dimens. (mm)	0.08x0.15x0.18	0.08x0.12x0.16	0.08x0.10x0.12	0.10 x 0.14x0.16	0.12 x0.16 x 0.18
θ range for data coll. (deg)	2.3- 27.5	2.0- 27.5	1.6 - 24.5	1.6-26.4	1.3-23.2
GOF	0.74	0.90	1.01	0.92	0.87
reflns. collected	21535	14342	10094	18681	16587
Uniq. reflns.	3760	3715	2962	5784	5724
final *R* indices [$I > 2\sigma(I)$]	R =0.0224 wR2 =0.0665	R = 0.0278 wR2 = 0.0787	R = 0.0470 wR2 = 0.0941	R = 0.0378 wR2 = 0.1137	R =0.0521 wR2 = 0.1449

Table S6. Selected bond parameters of the complexes **1c**, **1e**, **1f**, **1h** and **Pd-I**.

Bond Parameters	**1c**	**Bond Parameters**	**1e**	**1f**	**1h**	**Bond Parameters**	**Pd-I**
Pd1-Cl1	2.3219(9)	Pd1-Cl2	2.3219(10)	2.312(2)	2.3424(18)	Pd1-Cl2	2.383(2)
Pd1-N1	2.004(2)	Pd1-N1	2.003(2)	1.993(5)	2.002(4)	Pd1-P1	2.324(2)
Pd1-N3	1.9197(18)	Pd1-N3	1.917(2)	1.910(5)	1.925(4)	Pd1-P2	2.315(2)
Pd1-N4	2.100(2)	Pd1-N4	2.090(2)	2.094(5)	2.069(4)	Pd1-C11	1.989(7)
N2-N3	1.329(3)	N2-N3	1.329(3)	1.329(7)	1.328(6)	N2-N3	1.229(8)
N3-C6	1.378(3)	N3-C6	1.378(3)	1.378(8)	1.379(6)	Cl2 -Pd1-P1	90.69(6)
C11-N4	1.481(3)	C11-N4	1.485(4)	1.482(8)	1.477(6)	Cl2 -Pd1-P2	92.17(6)
N1-Pd1-N3	78.86(9)	N1-Pd1-N3	79.02(10)	79.0(2)	79.69(16)	Cl2-Pd1-C11	171.77(19)
Cl1-Pd1-N1	99.45(6)	Cl2-Pd1-N1	99.22(8)	99.49(14)	97.45(11)	P1 -Pd1-P2	175.10(6)
Cl1-Pd1-N4	97.69(5)	Cl2-Pd1-N4	97.52(7)	97.55(15)	98.93(12)	-	-
N3-Pd1-N4	84.00(8)	N3-Pd1-N4	84.23(9)	84.0(2)	83.94(17)	-	-

Table S7. Geometrical parameters of the complex **1c** (Å, °).

D–H···A	d(D–H)	d(H···A)	d(D···A)	D–H···A	Symmetry
C1–H1···Cl2	0.96	2.72	3.653(3)	165	1/2-x, -1/2+y, 1/2-z
C14–H14···Cg(4)	0.93	2.61	3.467(3)	154	1/2-x, 1/2-y, 1-z

Cg(4) is ring centroid of the C(6)–C(11) ring.

Table S8. Geometrical parameters (Å, º) for the π-stacking interactions.

rings *i-j*	Rc[a]	R1v[b]	R2v[c]	α[d]	β[e]	γ[f]	Symmetry
Cg(*3*)···Cg(*3*)	4.128(2)	4.018(2)	4.018(2)	0.0	13.28	13.28	1-x, 1-y, 1-z
Cg(*3*)···Cg(*4*)	3.840(2)	3.306(2)	3.392(2)	2.85	27.98	30.57	1-x, -y, 1-z

Cg(*3*) and Cg(*4*) are the centroids of the (N1/C1–C5) and (C6–C11) rings respectively. [a]Centroid distance between ring i and ring j. [b]Vertical distance from ring centroid i to ring j. [c]Vertical distance from ring centroid j to ring i. [d] Dihedral angle between the first ring mean plane and the second ring mean plane of the partner molecule. [e]Angle between centroids of first ring and second ring mean planes. [f] Angle between the centroid of the first ring and the normal to the second ring mean plane of the partner molecule.

Figure S1. Segmented cyclic voltammograms of [Pd(L^{1a-1f})Cl_2] in acetonitrile solution.

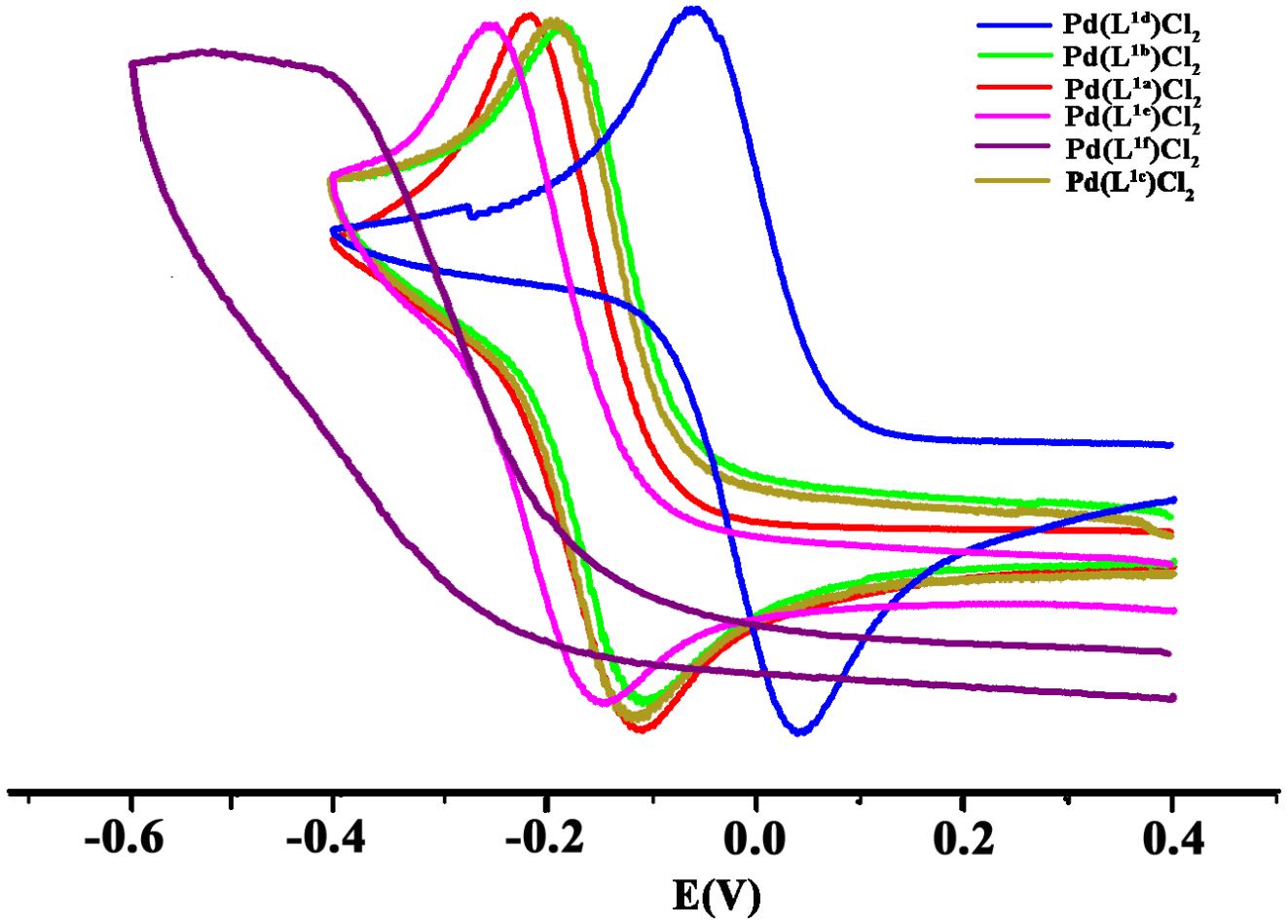

Figure S2. EPR spectra of the complexes (a) **1a** (b) **1f** (c) **1g** at 120 K.

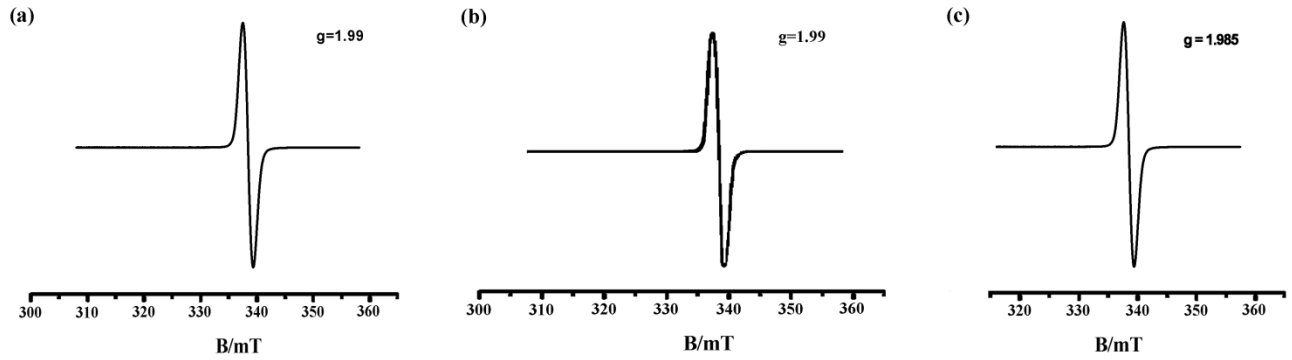

Figure S3. ORTEP representation of the complex **1c** at 50% probability ellipsoid.

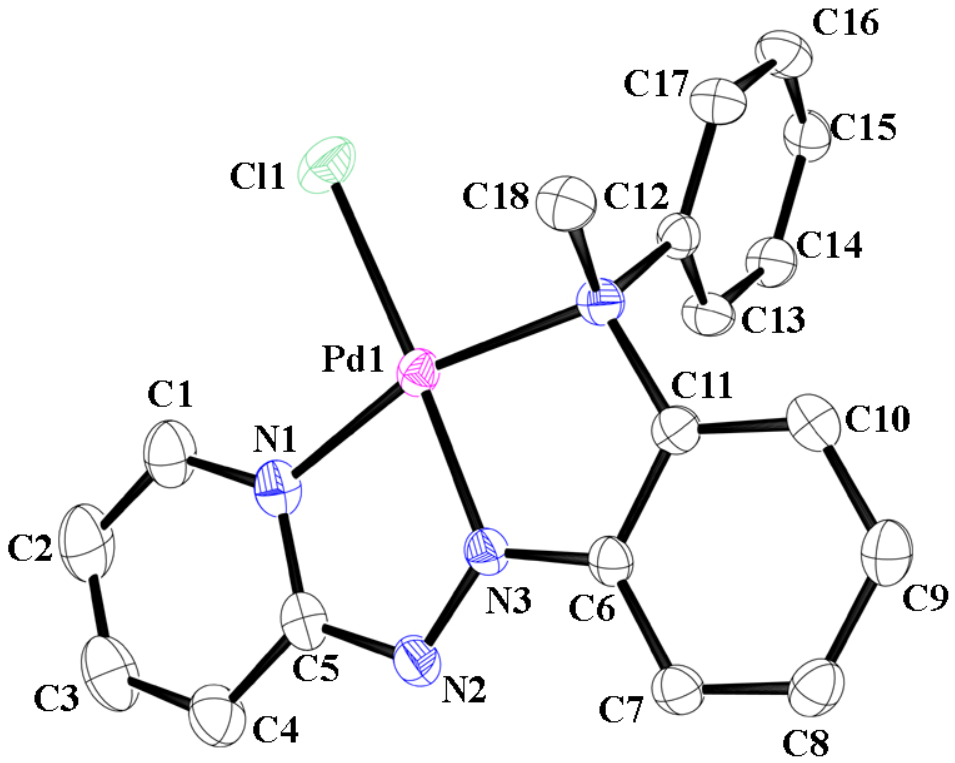

Figure S4. ORTEP representation of the complex **1e** at 50% probability ellipsoid.

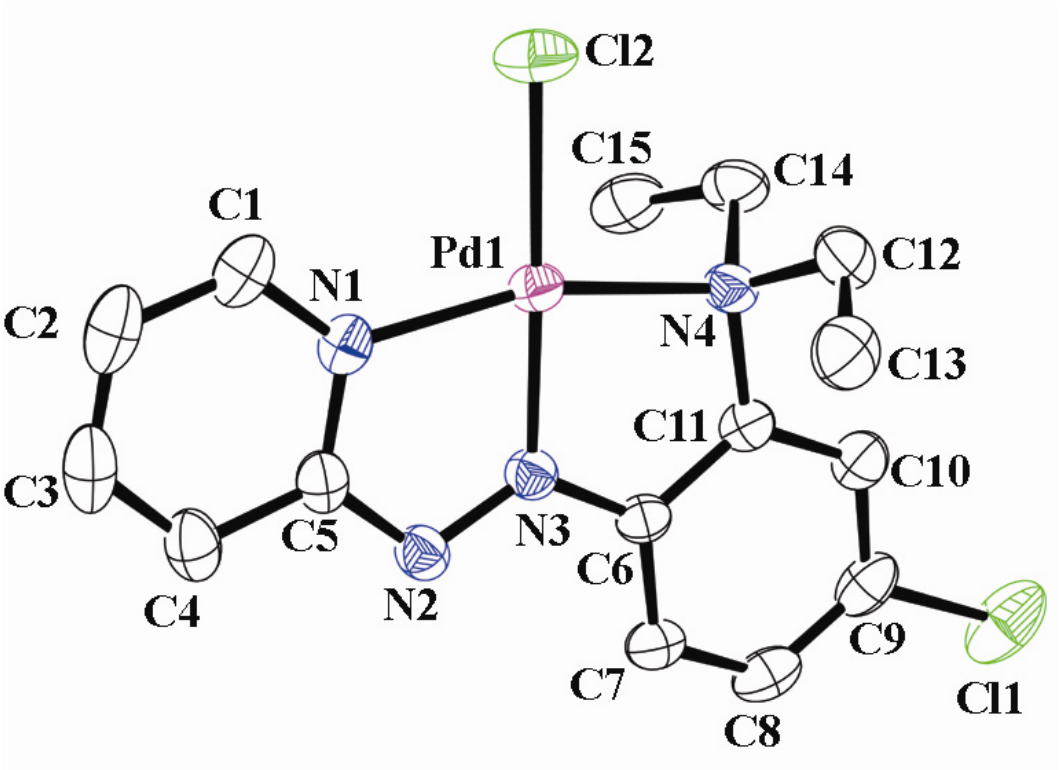

Figure S5. ORTEP representation of the complex **1f** at 50% probability ellipsoid.

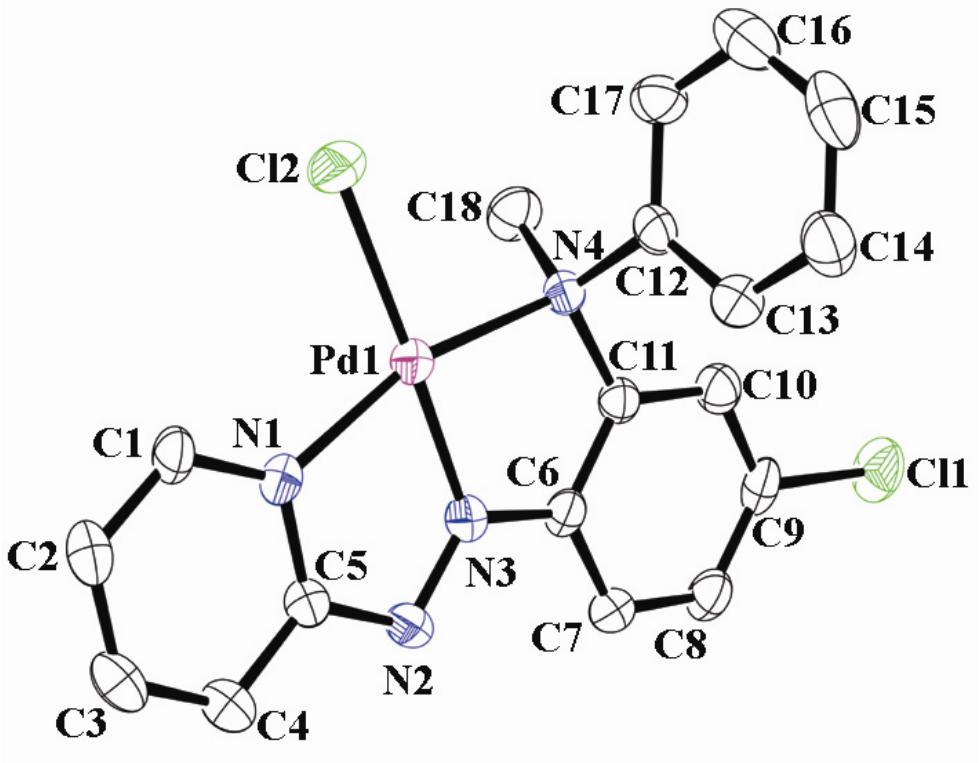

Figure S6. ORTEP representation of the complex **1h** at 50% probability ellipsoid.

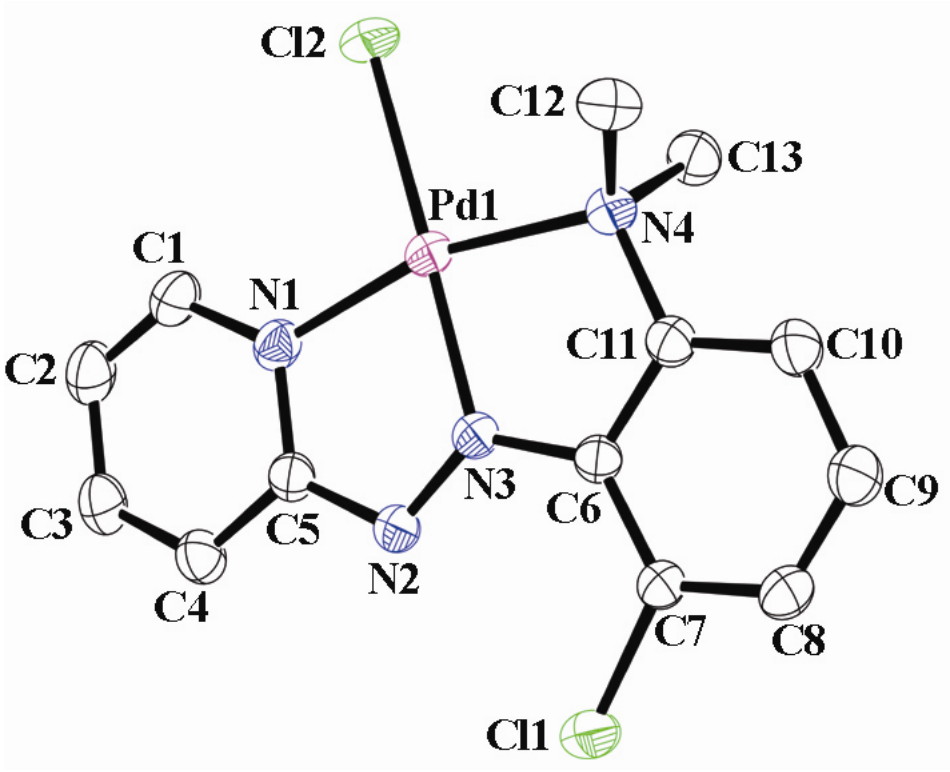

Figure S7**.** Formation of dimeric motif structure through C–H···π interactions in **1c**.

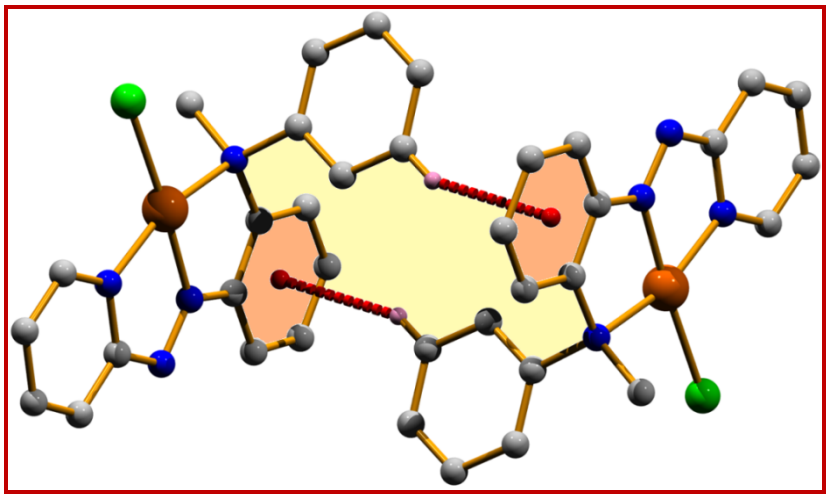

Figure S8. Two-dimensional supramolecular network generated through C–H···π and π–π stacking interactions in the (1 0 1) plane in **1c**.

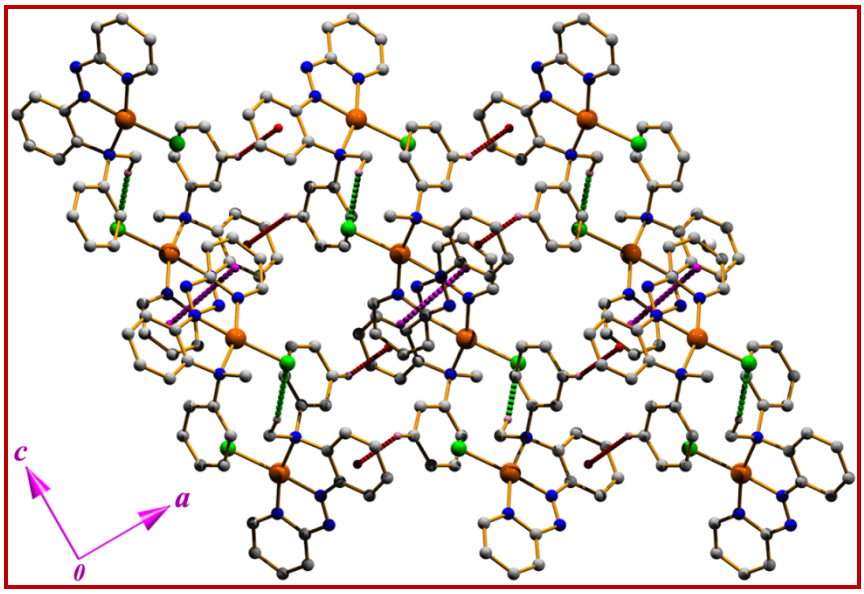

Figure S9. Cyclic voltammogram of the complex **1a** in dichloromethane solution.

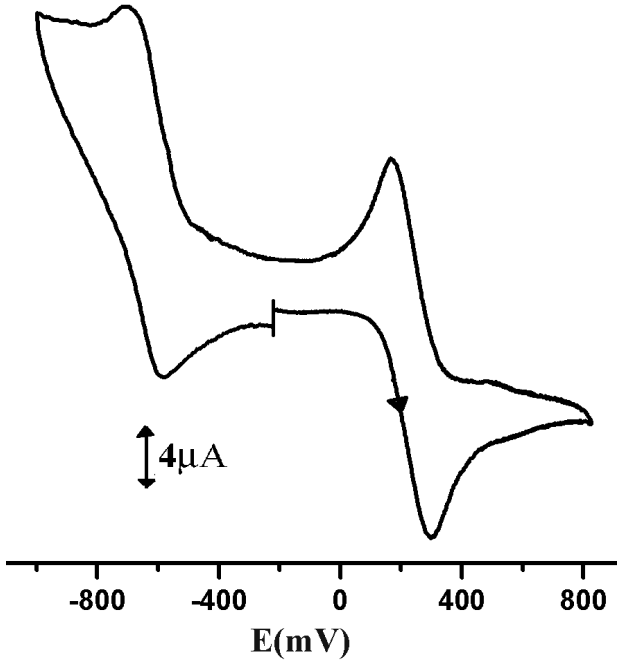

Figure S10. Cyclic voltammogram of the complex **1b** in dichloromethane solution.

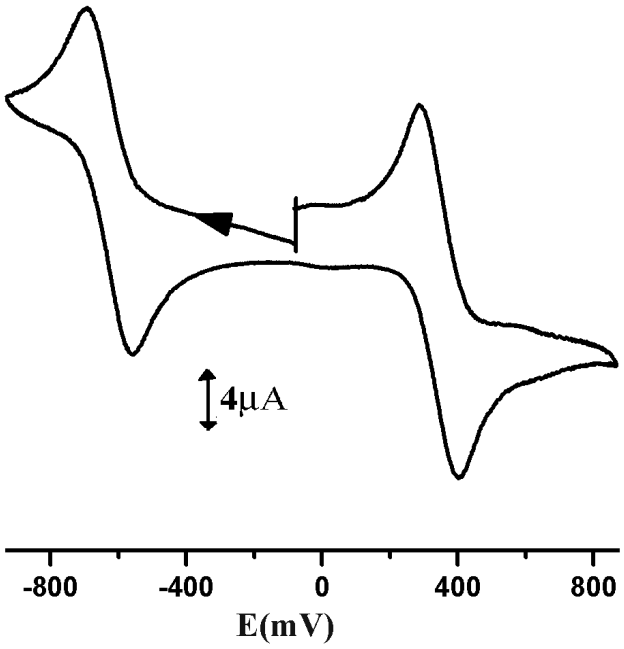

Figure S11. Cyclic voltammogram of the complex **1d** in dichloromethane solution.

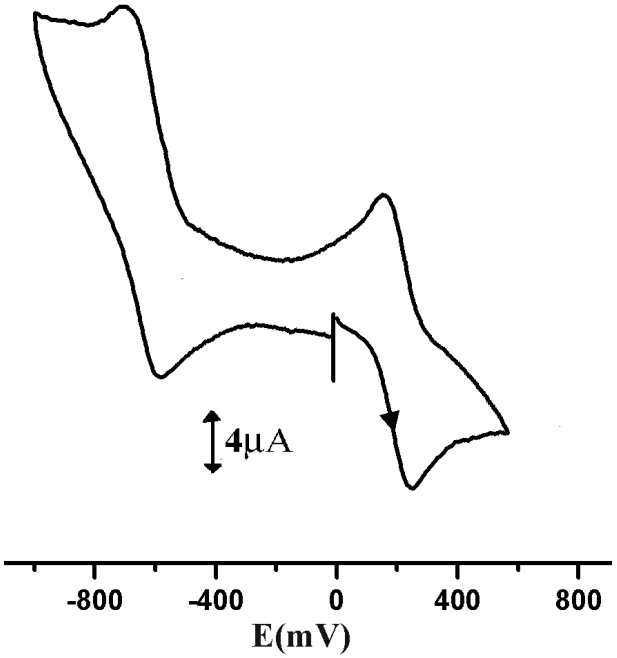

Figure S12. Cyclic voltammogram of the complex **1e** in dichloromethane solution.

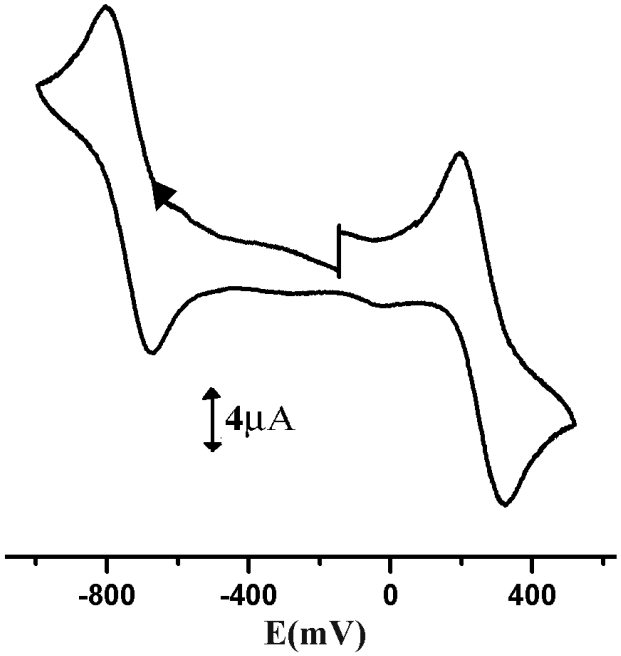

Figure S13. Cyclic voltammogram of the complex **1f** in dichloromethane solution.

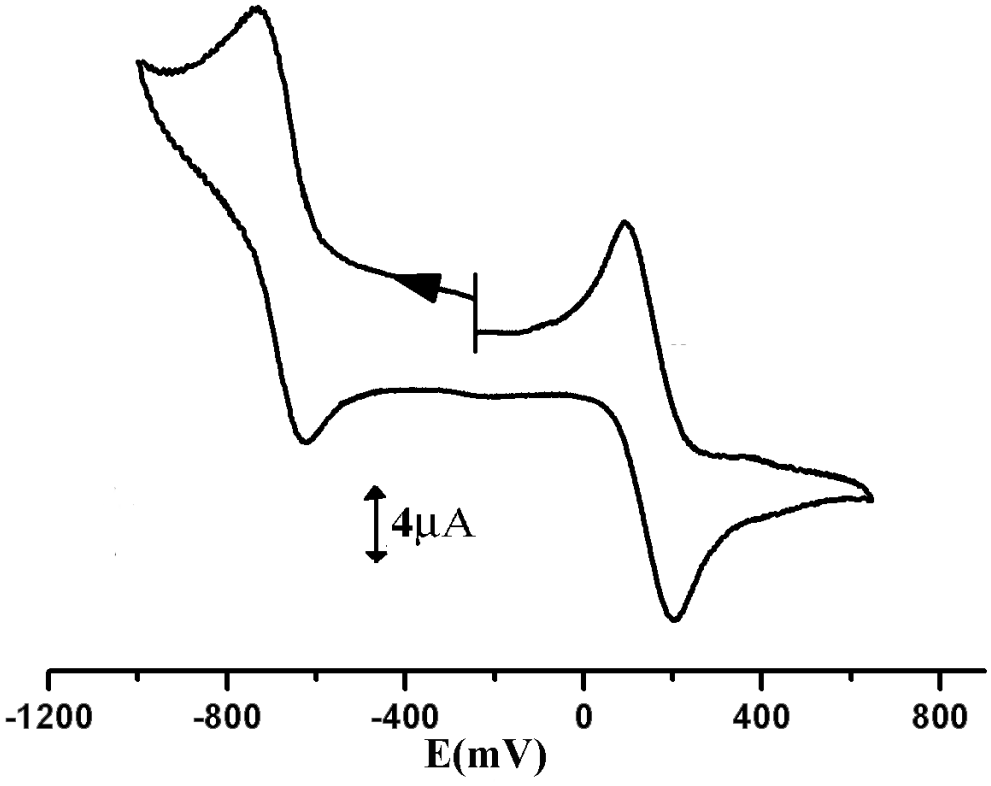

Figure S14. Cyclic voltammogram of the complex **1g** in dichloromethane solution.

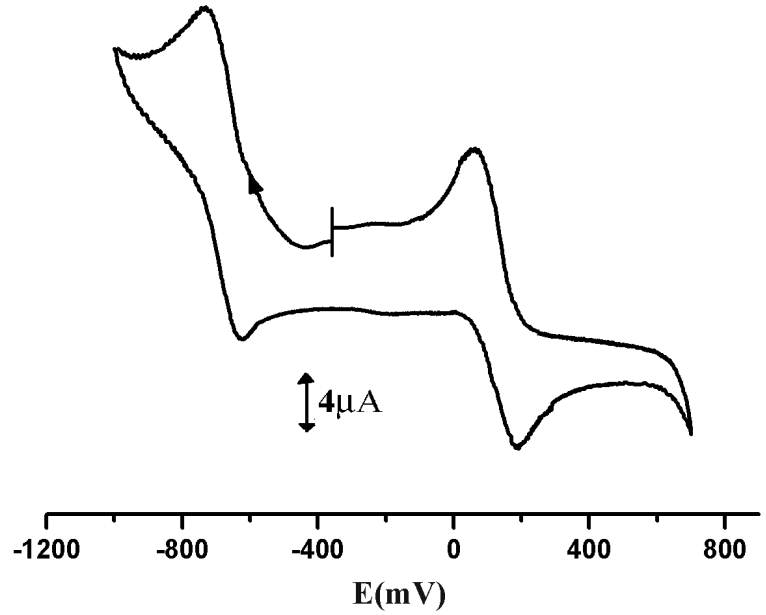

Figure S15. Cyclic voltammogram of the complex **1h** in dichloromethane solution.

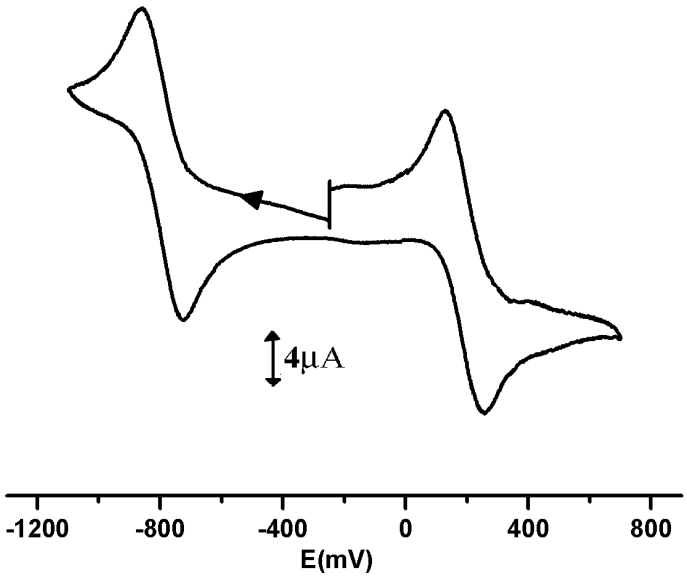

Figure S16. ^{1}H NMR spectrum of oxidized complex [**1f**]$^{+}$ in $CDCl_3$ solution. Inset: expansion of aromatic region.

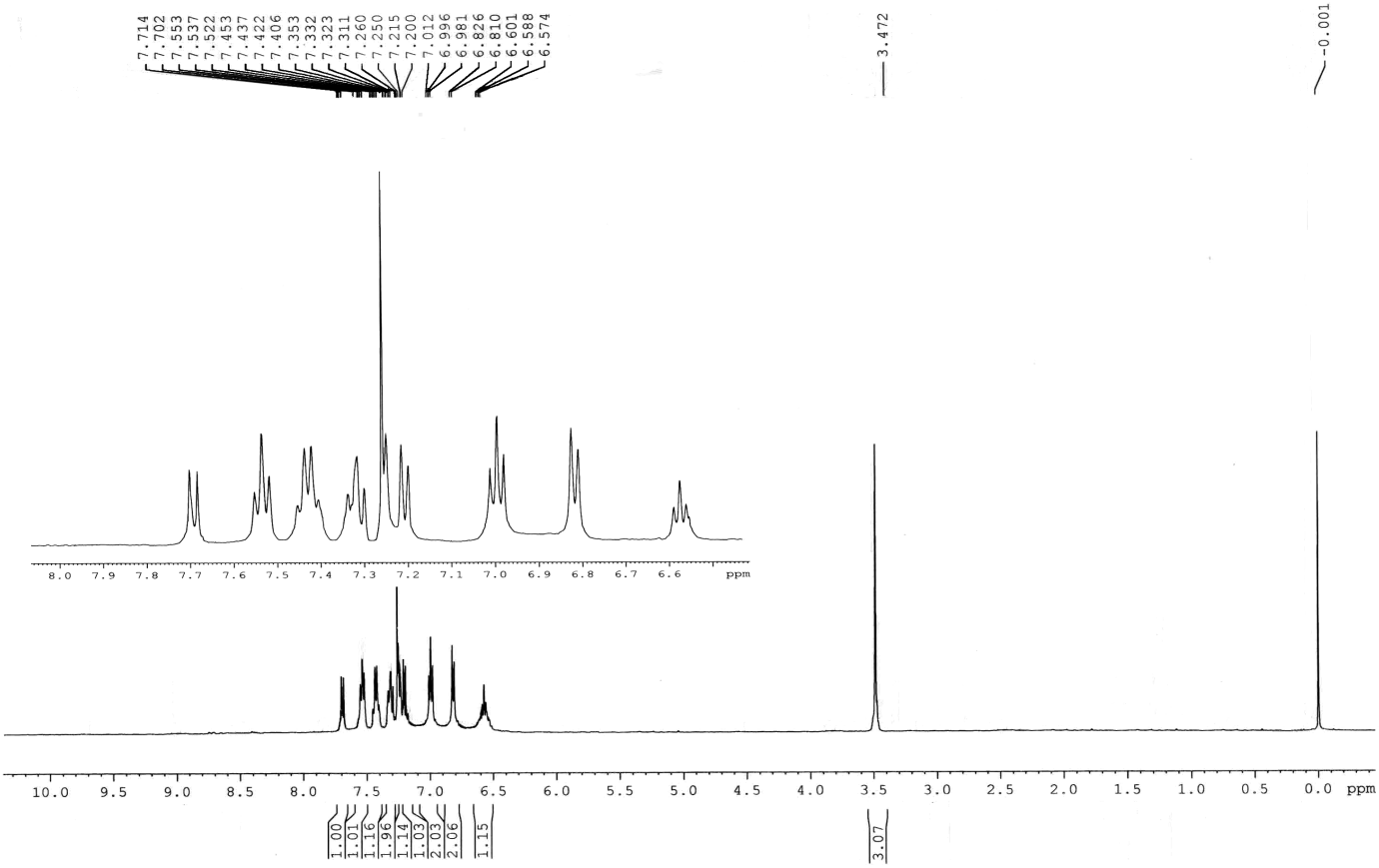

Figure S17. UV-vis spectra of complex **1a** – **1h** in dichloromethane solution.

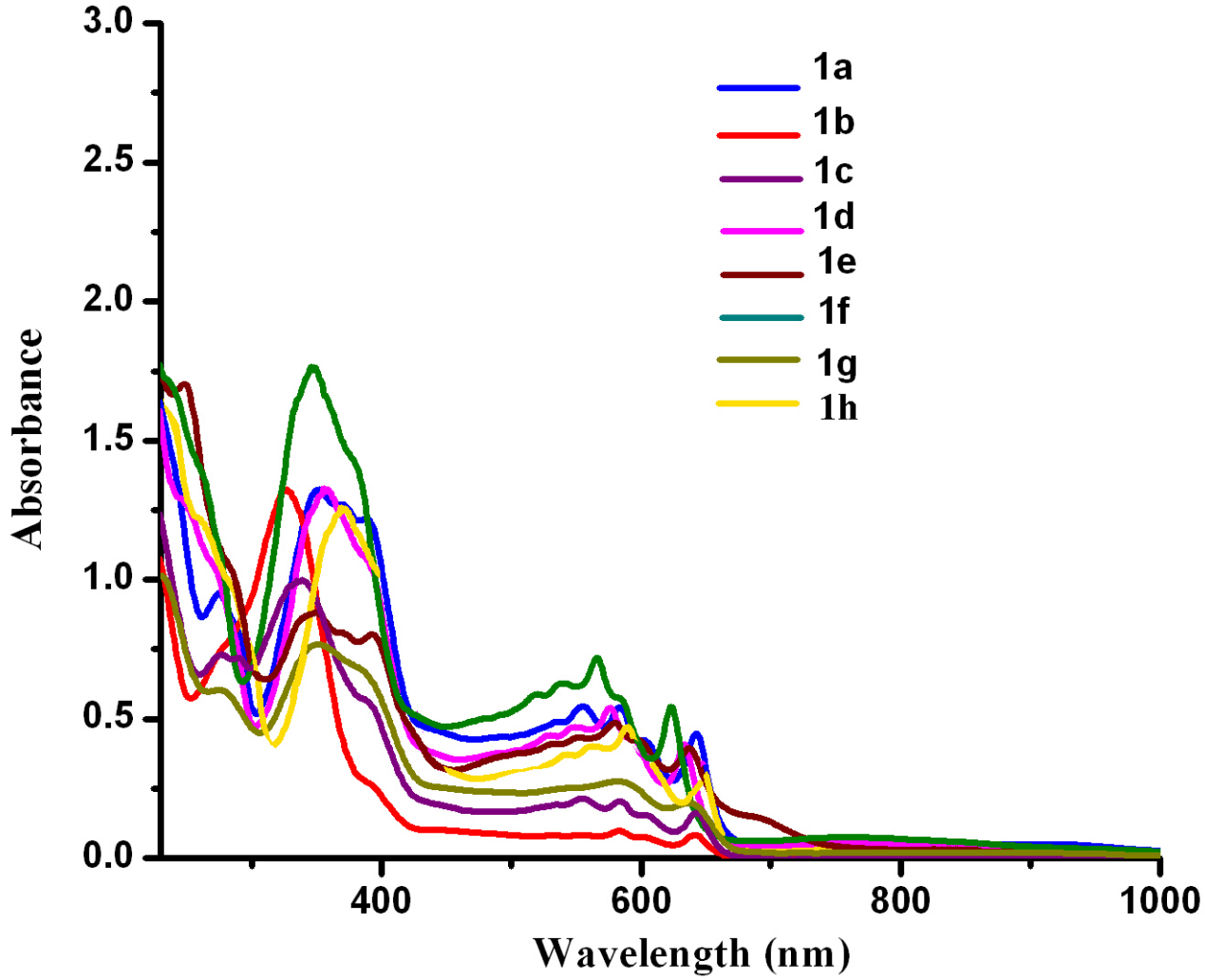

Figure S18. EPR spectrum of intermediate **I** (for $[Pd(L^{1b})Cl_2]^-$)at 120K.

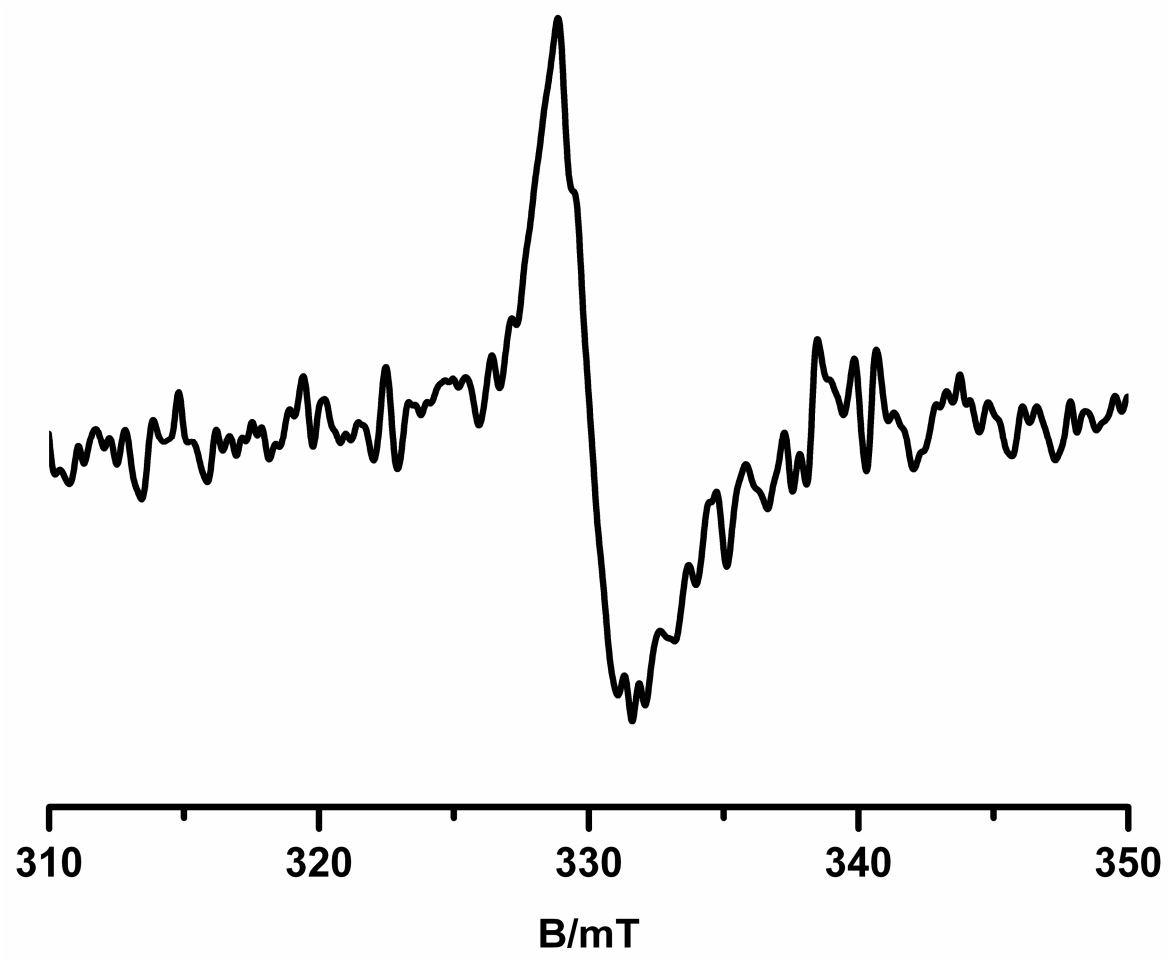

Figure S19. Mass spectrum of intermediate **I** (for $[Pd(L^{1b})Cl_2]^-$): (a) negative ion mode. (b) positive ion mode.

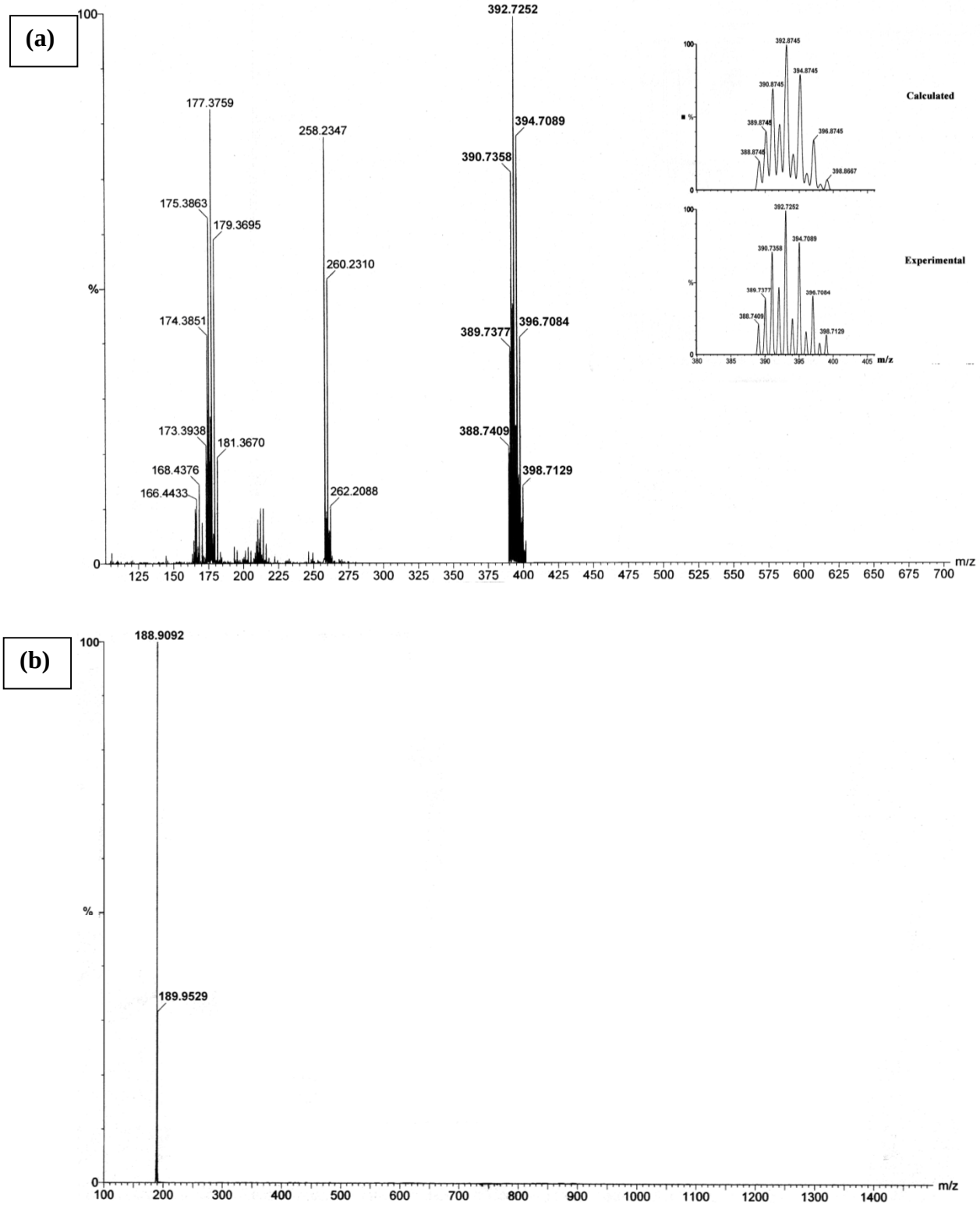

Figure S20. Chromatogram of isolated chlorobenzene from reaction between $Pd(L^{1d})Cl_2$ and triphenylamine.

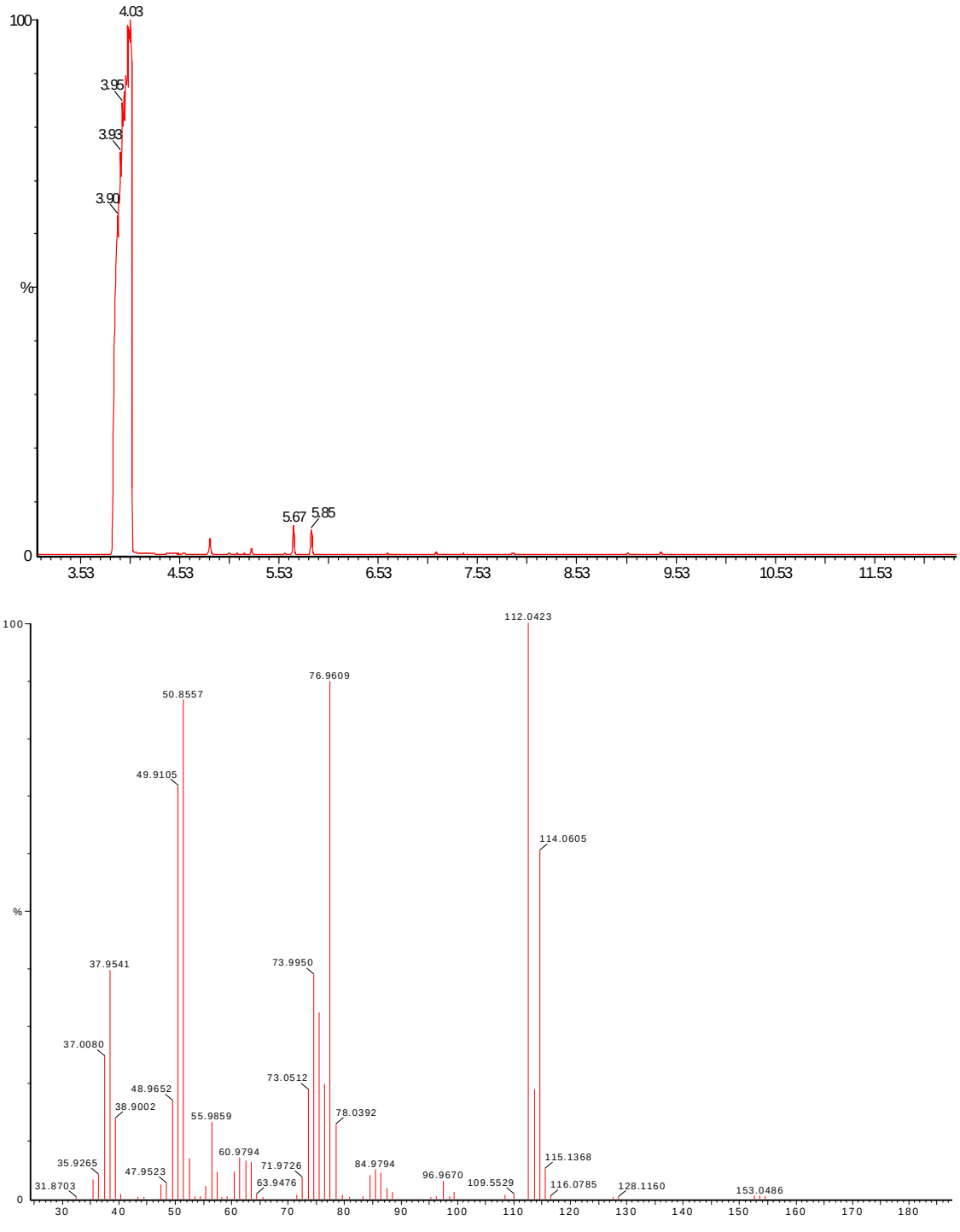

Figure S21. UV-vis spectra of coloumetrically reduced complexes $[Pd(L^1)Cl_2]^-$ in acetontrile solution.

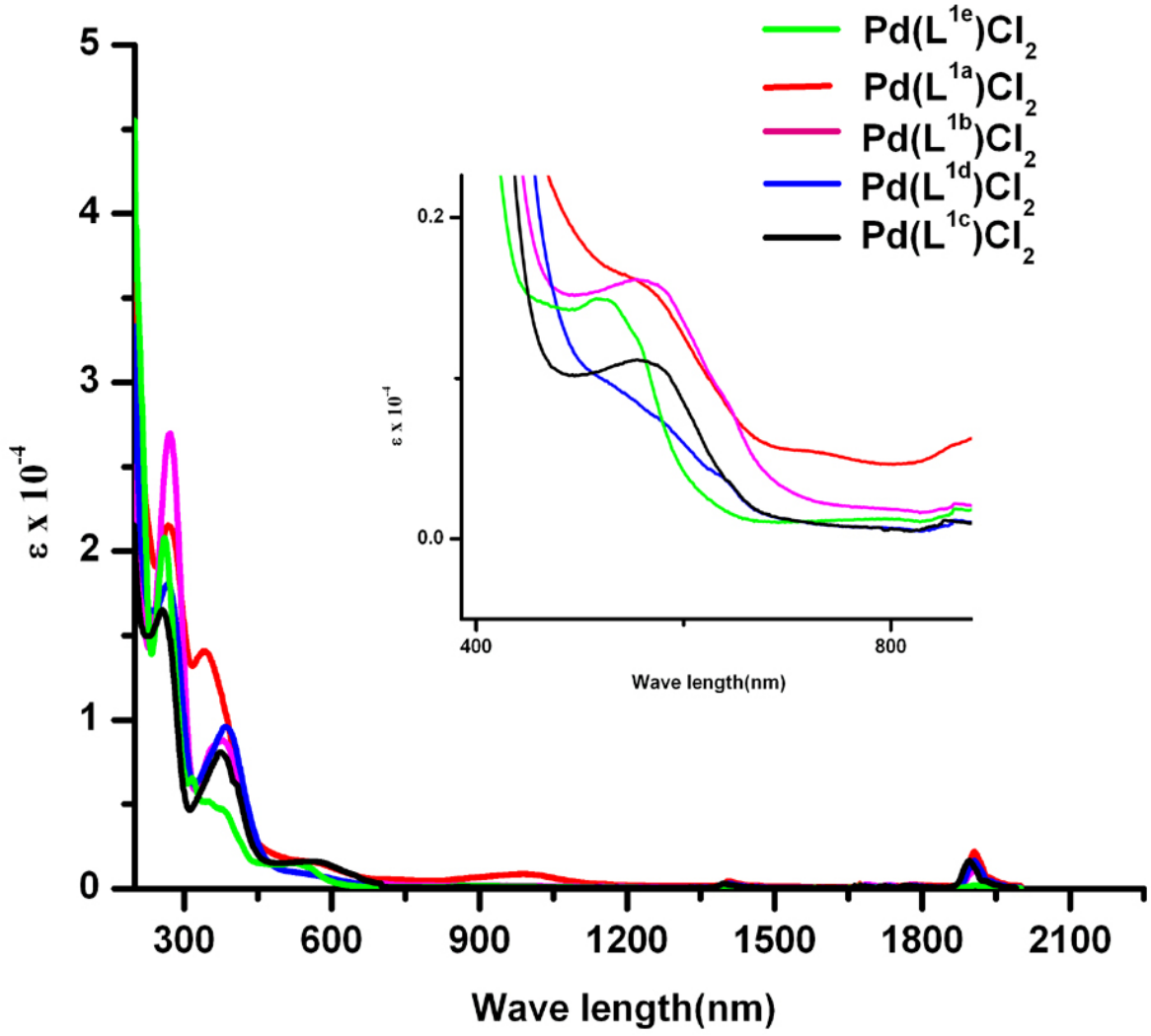

COMPUTATIONAL PART

Computational methods. All DFT calculations presented herein were carried out using the Gaussian 09 program package.[1] Geometry optimizations were performed without imposing geometric constraints (C_1 symmetry), and stationary points were subsequently confirmed to be minima by vibrational analysis (no imaginary frequencies). All calculations utilized the B3LYP hybrid functional.[2] The SDD basis set[3] was used on Pd and for C, H, N, polarized 6-31G (d) basis sets[4] was used. The TZVP basis set of triple-ζ quality with one set of polarization functions was used on Cl atom.[3] Mulliken spin densities were used for analysis of spin populations on ligand and metal centers.[5] Vertical electronic excitations based on B3LYP optimized geometries were computed using the time-dependent density functional theory (TD-DFT) formalism[6] in acetonitrile using conductor-like polarizable continuum model (CPCM).[7] GaussSum[8] was used to calculate the fractional contributions of various groups to each molecular orbital.

References:

1. Frisch, M. J.; Trucks, G. W.; Schlegel, H. B.; Scuseria, G. E.; Robb, M. A.; Cheeseman, J. R.; Montgomery, J. A., Jr.; Vreven, T.; Kudin, K. N.; Burant, J. C.; Millam, J. M.; Iyengar, S. S.; Tomasi, J.; Barone, V.; Mennucci, B.; Cossi, M.; Scalmani, G.; Rega, N.; Petersson, G. A.; Nakatsuji, H.; Hada, M.; Ehara, M.; Toyota, K.; Fukuda, R.; Hasegawa, J.; Ishida, M.; Nakajima, T.; Honda, Y.; Kitao, O.; Nakai, H.; Klene, M.; Li, X.; Knox, J. E.; Hratchian, H. P.; Cross, J. B.; Bakken, V.; Adamo, C.; Jaramillo, J.; Gomperts, R.; Stratmann, R. E.; Yazyev, O.; Austin, A. J.; Cammi, R.; Pomelli, C.; Ochterski, J. W.; Ayala, P. Y.; Morokuma, K.; Voth, G. A.; Salvador, P.; Dannenberg, J. J.; Zakrzewski, V. G.; Dapprich, S.; Daniels, A. D.; Strain, M. C.; Farkas, O.; Malick, D. K.; Rabuck, A. D.; Raghavachari, K.; Foresman, J. B.; Ortiz, J. V.; Cui, Q.; Baboul, A. G.; Clifford, S.; Cioslowski, J.; Stefanov, B. B.; Liu, G.; Liashenko, A.; Piskorz, P.; Komaromi, I.; Martin, R. L.; Fox, D. J.;

Keith, T.; Al-Laham, M. A.; Peng, C. Y.; Nanayakkara, A.; Challacombe, M.; Gill, P. M. W.; Johnson, B.; Chen, W.; Wong, M. W.; Gonzalez, C.; Pople, J. A. Gaussian 09, revision A.02; Gaussian, Inc.: Wallingford, CT, **2010**.

2. (a) Becke, A. D. *J. Chem. Phys*. **1993**, *98*, 5648; (b) Lee, C.; Yang W.; Parr R. G. *Phys. Rev. B: Condens. Matter*. **1988**, *37*, 785; (c) Vosko, S. H.; Wilk, L.; Nusair, M. *Can. J. Phys.* **1980**, *58*, 1200; (d) Stephens, P. J.; Devlin, F. J.; Chabalowski C. F.; Frisch, M. J. *J. Phys. Chem.* **1994**, *98*, 11623.

3. Schäfer, A.; Huber C.; Ahlrichs, R. *J. Chem. Phys.* **1994**, *100*, 5829.

4. Schäfer, A.; Horn H.; Ahlrichs, R. *J. Chem. Phys.* **1992**, *97*, 2571.

5. Mulliken, R. S. *J. Chem. Phys.* **1955**, *23*, 1833.

6. (a) Bauernschmitt, R.; Ahlrichs, R. *Chem. Phys. Lett.* **1996**, *256*, 454. (b) Stratmann, R. E.; Scuseria, G. E.; Frisch M. J. *J. Chem. Phys.* **1998**, *109*, 8218. (c) Casida, M. E.; Jamoroski, C.; Casida, K. C.; Salahub, D. R. *J. Chem. Phys.* **1998**, *108*, 4439.

7. (a) Cossi, M.; Rega, N.; Scalmani, G.; Barone, V. *J. Comput. Chem.* **2003**, *24*, 669. (b) Cossi, M.; Barone, V.; *J. Chem. Phys.* **2001**, *115*, 4708. (c) Barone, V.; Cossi, M. *J. Phys. Chem. A* **1998**, *102*, 1995. (d) O'Boyle, N. M.; Tenderholt, A. L.; Langner, K. M. *J. Comput. Chem.* **2008**, *29*, 839.

8. Leininger, T.; Nicklass, A.; Stoll, H.; Dolg, M.; Schwerdtfeger, P. J. *J. Chem. Phys.* **1996,** *105*, 1052.

Figure S22. (a) Contour plots of HOMO and LUMO of [**1c**]$^{+}$.

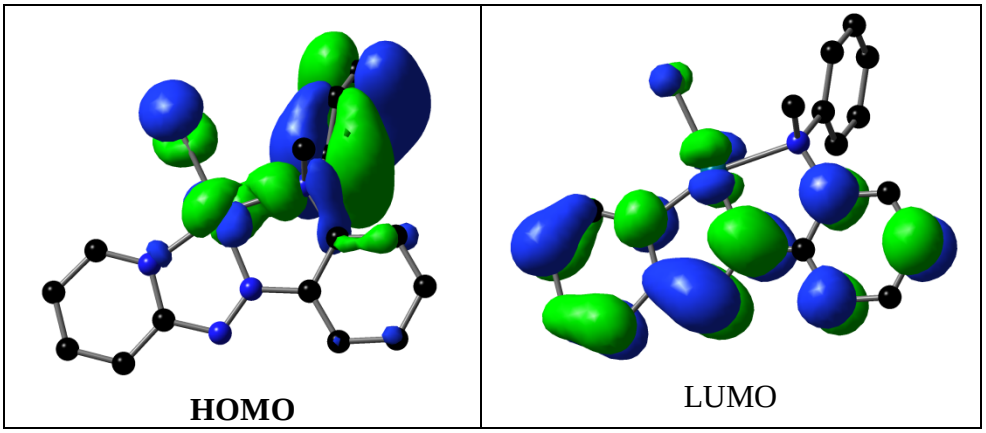

Figure S22. (b) Contour plots of HOMO and LUMO of [**1c**]$^{-}$.

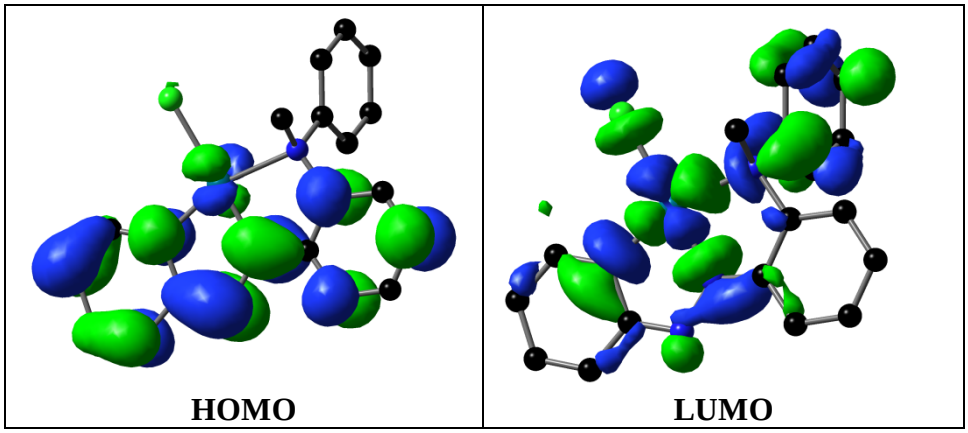

Cartesian coordinates of complex **1c**

Pd	4.680500	2.154500	6.025300
Cl	4.740400	2.742000	3.738800
C	-0.477900	2.787800	4.761600
H	-1.373000	3.326700	4.465100
C	6.963200	4.201100	6.058700
H	6.737500	4.306100	5.002600
C	3.512600	-0.379300	5.034500
H	4.388600	-0.849100	5.482200
H	3.792400	0.049700	4.072300
H	2.722300	-1.128300	4.905400
C	2.003600	-0.776300	7.664300
H	1.305700	-1.121200	6.907000
C	7.964900	4.924000	6.689300
H	8.558100	5.630600	6.120000
N	3.065500	0.715100	5.951500
N	4.731600	1.644700	7.913400
C	0.155700	1.928900	3.867400
H	-0.238700	1.794800	2.864200
N	5.622400	2.189800	8.727400
C	1.308400	1.231500	4.240300
H	1.788900	0.588600	3.514700
C	3.778000	0.151300	9.633500
H	4.470600	0.529300	10.376200
C	2.953300	0.186400	7.338600

C	2.830500	-0.817300	9.939700
H	2.780100	-1.212300	10.950700
N	6.199700	3.313600	6.720600
C	6.396900	3.090700	8.076700
C	1.834800	1.396900	5.523500
C	3.845500	0.667600	8.323700
C	1.939200	-1.284100	8.964500
H	1.197200	-2.036400	9.213700
C	0.054100	2.953300	6.043400
H	-0.423800	3.623400	6.752600
C	1.202100	2.265500	6.424700
H	1.611200	2.404700	7.419700
C	7.408200	3.807500	8.756700
H	7.545700	3.618100	9.815100
C	8.183600	4.716800	8.063700
H	8.961600	5.270400	8.581800

Cartesian coordinates of complex [**1c**]$^{+}$

Pd	4.662800	2.166000	6.027600
Cl	4.685000	2.794000	3.807200
C	-0.492200	2.758400	4.753300
H	-1.393300	3.285700	4.456100
C	6.953700	4.239400	6.075400
H	6.727100	4.383200	5.024000
C	3.537400	-0.372900	5.032600
H	4.428400	-0.822800	5.471700
H	3.789500	0.047800	4.060000
H	2.755800	-1.132100	4.931200
C	1.989900	-0.734600	7.650300
H	1.276000	-1.061100	6.901400
C	7.968700	4.941800	6.735300
H	8.558400	5.664500	6.182200
N	3.081100	0.736700	5.939700
N	4.769100	1.628000	7.909700
C	0.101700	1.841800	3.887900
H	-0.331500	1.651800	2.910900
N	5.621100	2.148000	8.693500
C	1.262600	1.157400	4.259100
H	1.707400	0.463900	3.557500
C	3.796900	0.133800	9.630400
H	4.499300	0.493400	10.373800
C	2.960000	0.208400	7.324800

C	2.833300	-0.817700	9.934300
H	2.774000	-1.224400	10.938500
N	6.199300	3.341300	6.717100
C	6.419700	3.094300	8.049300
C	1.830000	1.400900	5.511100
C	3.854600	0.645800	8.324000
C	1.932700	-1.247200	8.948800
H	1.177000	-1.986900	9.194100
C	0.081600	2.996900	6.004900
H	-0.369700	3.710100	6.687800
C	1.239400	2.324100	6.385400
H	1.679600	2.521100	7.358000
C	7.415500	3.760500	8.760500
H	7.556200	3.533500	9.810900
C	8.200400	4.700100	8.087800
H	8.982700	5.234100	8.617500

Cartesian coordinates of complex [**1c**]$^-$

Pd	4.676600	2.197500	6.036200
Cl	4.779300	2.718200	3.665000
C	-0.522900	2.764300	4.756200
H	-1.425200	3.293400	4.460200
C	7.014200	4.161400	6.063500
H	6.799000	4.240500	5.002100
C	3.509400	-0.342800	5.034400
H	4.387200	-0.798900	5.492800
H	3.799000	0.099700	4.079900
H	2.738100	-1.111000	4.883400
C	2.005800	-0.785200	7.672800
H	1.319200	-1.142400	6.907700
C	8.022300	4.879500	6.669400
H	8.641500	5.552900	6.086200
N	3.030700	0.723300	5.956500
N	4.623700	1.753800	7.942800
C	0.139400	1.936300	3.854600
H	-0.239000	1.815500	2.842300
N	5.602800	2.261000	8.771600
C	1.300700	1.252600	4.228700
H	1.805800	0.636200	3.496800
C	3.779800	0.162700	9.625200
H	4.473600	0.541700	10.366300
C	2.929700	0.198700	7.345300

C	2.857800	-0.828300	9.926000
H	2.838800	-1.237400	10.935500
N	6.221600	3.294500	6.731600
C	6.381300	3.095700	8.124100
C	1.814300	1.395200	5.522100
C	3.826800	0.728600	8.318100
C	1.952600	-1.313900	8.967600
H	1.232900	-2.088300	9.217600
C	-0.004300	2.912400	6.047500
H	-0.500100	3.562000	6.764700
C	1.150000	2.238000	6.429100
H	1.553700	2.362600	7.427800
C	7.428100	3.838000	8.778100
H	7.550800	3.689300	9.846300
C	8.220500	4.697900	8.068900
H	9.005900	5.252300	8.580600